# Trimeric Subunit Stoichiometry of the Glutamate Transporters from *Bacillus caldotenax* and *Bacillus stearothermophilus*†

Dinesh Yernool,‡,§ Olga Boudker,‡,§,|| Ewa Folta-Stogniew,⊥ and Eric Gouaux*,§,||

*Department of Biochemistry and Molecular Biophysics and Howard Hughes Medical Institute, 650 West 168th Street, Columbia University, New York, New York 10032, and HHMI Biopolymer Laboratory and W. M. Keck Foundation Biotechnology Resource Laboratory, Yale University, New Haven, Connecticut 06520*

*Received June 30, 2003; Revised Manuscript Received August 28, 2003*

ABSTRACT: Catalysis of glutamate transport across cell membranes and coupling of the concentrative transport to sodium, proton, and potassium gradients are processes fundamental to organisms in all kingdoms of life. In bacteria, glutamate transporters participate in nutrient uptake, while in eukaryotic organisms, the transporters clear glutamate from the synaptic cleft. Even though glutamate transporters are crucial to the viability of many life forms, little is known about their structure and quaternary organization. In particular, the subunit stoichiometry of these polytopic integral membrane proteins has not been unequivocally defined. Determination of the native molecular mass of membrane proteins is complicated by their lability in detergent micelles and by their association with detergent and/or lipid molecules. Here we report the purification of glutamate transporters from *Bacillus caldotenax* and *Bacillus stearothermophilus* in a monodisperse, detergent-solubilized state. Characterization of both transporters either by chemical cross-linking and mass spectrometry or by size-exclusion chromatography and in-line laser light scattering, refractive index, and ultraviolet absorption measurements shows that the transporters have a trimeric quaternary structure. Limited proteolysis further defines regions of primary structure that are exposed to aqueous solution. Together, our results define the subunit stoichiometry of high-affinity glutamate transporters from *B. caldotenax* and *B. stearothermophilus* and localize exposed and accessible elements of primary structure. Because of the close amino acid sequence relationship between bacterial and eukaryotic transporters, our results are germane to prokaryotic and eukaryotic glutamate and neutral amino acid transporters.

The selective, vectorial transport of chiral molecules bearing multiple charges across a membrane bilayer and against a concentration gradient is a complex molecular process. While much progress has been made in understanding the comparatively simple process of monovalent ion permeation and gating (*1*, *2*), there is relatively little information on the structure and organization of molecular transporters. One particularly important and widespread type of molecular transporter is glutamate transporters (*3*−*6*), members of the dicarboxylate/amino acid:cation ($Na^+$ or $H^+$) symporter (DAACS)[1] family (*7*). These transporters couple the movement of glutamate, aspartate, selected neutral amino acids, or dicarboxylic acids to the cotransport of sodium ions and/or protons and the countertransport of potassium (*7*). In eukaryotes, members of the DAACS family play a crucial role in the function of the central nervous system, clearing glutamate and aspartate from the synaptic cleft, and thus are known as excitatory amino acid transporters (EAAT), one of the two structurally distinct families of neurotransmitter transporters (*8*). Strikingly, both prokaryotic and eukaryotic members of the DAACS family share significant amino acid homology and functional properties including (i) coupling substrate transport against a concentration gradient by cotransporting sodium ions and/or protons, (ii) similar substrate specificities, and (iii) similar, experimentally determined transmembrane topology. Therefore, from both the analysis of amino acid sequence information and substantial functional data, the sodium-dependent, high-affinity glutamate transporters from prokaryotes and eukaryotes are closely related (*7*).

The bacterial, sodium-dependent glutamate transporters that have been characterized to date are from *Escherichia*

† E.G. is an assistant investigator with the Howard Hughes Medical Institute. D.Y. was supported by a NRSA postdoctoral fellowship (GM20547).

* To whom correspondence should be addressed. E-mail: jeg52@columbia.edu. Phone: (212) 305-4475. Fax: (212) 305-8174.

‡ These authors made equal contributions.

§ Department of Biochemistry and Molecular Biophysics, Columbia University.

|| Howard Hughes Medical Institute, Columbia University.

⊥ Yale University.

[1] Abbreviations: DAACS, dicarboxylate/amino acid:cation ($Na^+$ or $H^+$) symporter; EAAT, excitatory amino acid transporter; GLT-1, glutamate transporter 1; GLAST, L-glutamate/L-aspartate transporter 1; EAAC1, excitatory amino acid carrier 1; $GltT_{Bc}$, glutamate transporter from *Bacillus caldotenax*; $GltT_{Bs}$, glutamate transporter from *Bacillus stearothermophilus*; MBP, maltose binding protein; DM, *n*-dodecyl β-D-maltoside; SEC, size-exclusion chromatography; EDTA, ethylenediaminetetraacetic acid; TEV, tobacco etch virus; MALDI-MS, matrix-assisted laser desorption/ionization time-of-flight mass spectrometry; UV, ultraviolet; SEC-LS/UV/RI, SEC coupled with in-line light scattering, ultraviolet absorption, and refractive index detectors; MW, molecular weight; LL, long linker; SL, short linker; SDS−PAGE, sodium dodecyl sulfate−polyacrylamide gel electrophoresis; α-HL, α-hemolysin from *Staphylococcus aureus*; LamB, maltoporin from *Escherichia coli*; IPTG, isopropyl β-D-thiogalactoside.

10.1021/bi030161q CCC: $25.00 
Published on Web 10/18/2003

*coli*, *Bacillus caldotenax*, *Bacillus stearothermophilus*, and *Bacillus subtilus* (*9*). In eukaryotes, there are five distinct subtypes of sodium-dependent, high-affinity glutamate transporters (EAAT1−5) that have been cloned from a wide variety of organisms and that differ in their expression patterns and functional properties (*10*). While there are many common features that bind the prokaryotic and eukaryotic transporters, there is one property specific to the eukaryotic transporters. In particular, eukaryotic transporters possess a substantial, substrate-gated chloride conductance (*3*, *11*) which is thermodynamically uncoupled from the glutamate transport.

For both prokaryotic and eukaryotic glutamate transporters, a host of elegant experiments and analyses have revealed important relationships between the amino acid sequence and biological function and have defined substrate and inhibitor specificity, dependence upon cotransported and counter transported ions, kinetic mechanisms, and lipid-dependent modulation. Likewise, studies employing alkaline phosphatase fusion proteins, single cysteine mutants, and both the prokaryotic and eukaryotic transporters have shown that the amino and carboxy termini are cytoplasmic, that there are at least eight transmembrane segments, and that some residues, localized to reentrant loop-like elements, are accessible from the interior and exterior of the cell. Together, these studies have resulted in two closely related models for the transmembrane topology of glutamate transporters (*3*−*5*, *8*, *12*, *13*).

There is, however, little information on the subunit stoichiometry of glutamate transporters. No experimental data are available on the bacterial transporters, and the two extant studies on the eukaryotic transporters are contradictory. Indeed, determination of subunit stoichiometry of polytopic membrane proteins is a challenging task, not only because the proteins are often unstable and prone to aggregation and/or dissociation but also because standard methods for the determination of native molecular mass, such as sedimentation equilibrium studies by analytical ultracentrifugation, are not readily applied to membrane proteins due to the presence of unknown amounts of bound detergent and lipid. Nevertheless, cross-linking studies on the eukaryotic GLT-1 (EAAT2) and GLAST (EAAT1) transporters carried out on unpurified proteins in cell membranes indicated that GLT-1 and GLAST can be readily cross-linked as trimers and dimers, respectively (*14*). By contrast, a freeze−fracture electron microscopy study of EAAT3 overexpressed in *Xenopus* oocytes suggests that EAAT3 has a pentameric subunit stoichiometry (*15*). Because there is no consensus on the subunit stoichiometry of eukaryotic glutamate transporters, and there are no available data on bacterial glutamate transporters, which in principle should be the most amenable to characterization, we embarked on a comprehensive study using two different methods to determine the subunit stoichiometry of bacterial glutamate transporters.

Here we describe determination of the subunit stoichiometry of the high-affinity, sodium-dependent glutamate transporters from *B. caldotenax* ($GltT_{Bc}$) and *B. stearothermophilus* ($GltT_{Bs}$), two well-characterized bacterial transporters that retain transport activity following membrane extraction and purification (*16*−*20*). On the basis of glutaraldehyde cross-linking followed by mass spectrometry on one hand (*21*) and size-exclusion chromatography coupled with in-line laser light scattering, ultraviolet, and refractive index (SEC-LS/UV/RI) measurements on the other hand (*22*, *23*), we show that the bacterial transporters are trimers. We then further explore the accessibility of the transporter primary structure, subjecting the transporters to limited proteolysis, and define regions of the polypeptide that are sufficiently solvent exposed and accessible so as to be protease sensitive. Taken together, our studies demonstrate that SEC-LS/UV/RI is a powerful probe of the native molecular mass of membrane proteins, that bacterial glutamate transporters are trimers, and that the "loops" between transmembrane segments 3 and 4 and proximal to the conserved serine-rich region are flexible and accessible from aqueous solution. Because of significant amino acid sequence relationships between $GltT_{Bs}$/$GltT_{Bc}$ and eukaryotic glutamate and neutral amino acid transporters (*7*), the results reported here are relevant to understanding the eukaryotic glutamate and neutral amino acid transporters as well.

## EXPERIMENTAL PROCEDURES

*Expression Vectors.* The $gltT_{Bs}$ gene with an amino-terminal $His_6$ tag cloned into the pBAD24 vector and under control of an arabinose promoter (*His-*$gltT_{Bs}$) was a gift from D. Slotboom, W. N. Konings, and J. S. Lolkema (*24*). The $gltT_{Bc}$ gene was amplified by PCR from pGBT231 (*18*) and cloned into the pMBP-Parallel2 vector between *Nco*I and *Xho*I sites, under control of a $P_{tac}$ promoter (*25*), producing an amino-terminal fusion with maltose binding protein (MBP) via a short linker (*MBP-SL-*$gltT_{Bc}$). *MBP-SL-*$gltT_{Bc}$ was cut with *Nco*I, and an oligonucleotide encoding the peptide MSSGLVPRGSAGSRGA was inserted, yielding the long linker construct, *MBP-LL-*$gltT_{Bc}$. The $gltT_{Bc}$ gene was also subcloned from *MBP-SL-*$gltT_{Bc}$ into pBAD24 in place of $gltT_{Bs}$, giving *His-*$gltT_{Bc}$. The integrity of all constructs was verified by sequencing both strands of the DNA.

*Protein Expression and Purification.* The $His_6$-tagged proteins were expressed in *E. coli* Top10 cells as described previously (*24*), and the MBP fusions were expressed in DH5α cells following induction with 0.05 mM isopropyl β-D-thiogalactoside at 22 °C for 3 h. Crude membranes were isolated in 20 mM Tris-HCl, pH 7.4, 0.2 M NaCl, 5 mM sodium glutamate, and 1 mM EDTA (buffer 1). Membranes were solubilized in buffer 1 containing 40 mM *n*-dodecyl β-D-maltoside (DM). After 1 h, the DM was diluted to 10 mM prior to chromatography. For $His_6$-tagged proteins, EDTA was omitted from buffer 1.

All buffers used in subsequent purification steps contained 2 mM DM. His-$GltT_{Bc}$ and His-$GltT_{Bs}$ were purified on Ni-NTA resin followed by size-exclusion chromatography (SEC). MBP fusion proteins were purified using amylose resin (New England Biolabs) in buffer 1. MBP was cleaved from MBP-LL-$GltT_{Bc}$ by overnight digestion with a 1:16 (w/w) ratio of tobacco etch virus (TEV) protease to transporter. Cleaved LL-$GltT_{Bc}$ was then purified by SEC. Intrinsic *E. coli* maltoporin (LamB) was also purified by amylose affinity chromatography. Heptameric α-hemolysin (α-HL) was purified as described previously (*26*).

*Protein Characterization.* The identities of all purified proteins were confirmed by amino-terminal sequencing of the first eight amino acids and by matrix-assisted laser desorption/ionization time-of-flight mass spectrometry (MAL-

DI-MS). Protein concentration was determined from ultraviolet (UV) absorbance at 280 nm using extinction coefficients calculated from corresponding amino acid sequences (*27*). Analytical and preparative SEC was performed using Superose-6 HR (10/30) and Superdex 200 HiLoad (16/60) columns (Pharmacia Biotech), respectively. All SEC experiments were performed in buffer 1.

*Reconstitution and Flux Assays.* Proteoliposomes were prepared, and transport activity was assayed according to a previously developed protocol (*20*). Liposomes were prepared from a 3:1 (w/w) mixture of total *E. coli* lipid extract and egg lecitin. Purified transporter was reconstituted at protein to lipid ratio of 1:400 (w/w). Proteoliposomes were loaded with 50 mM potassium phosphate and 100 mM potassium acetate, pH 7.0. The external buffer contained 125 mM 2-(*N*-morpholino)ethanesulfonic acid titrated to pH 6.0 with *N*-methyl-D-glucamine and 0.1 $\mu$M sodium [$^3$H]-glutamate. Proteoliposomes were diluted into the external buffer 200−400-fold, and transport was assayed at 30 °C.

*Glutaraldehyde Cross-Linking and Analysis by SDS−PAGE and MALDI-MS.* Purified $GltT_{Bc}$ and $GltT_{Bs}$ were dialyzed extensively against 50 mM sodium phosphate and 100 mM NaCl, pH 7.4. Protein solutions at 0.25 mg/mL were incubated with glutaraldehyde at 25 °C for 30 min, and reactions were quenched with 100 mM Tris-HCl, pH 7.4, for 15 min prior to further analysis. To prepare samples for mass spectrometry, protein solutions were incubated with 2.5 mM glutaraldehyde. After the reactions were quenched, cross-linked protein samples were concentrated by ultrafiltration to at least 2 mg/mL. MALDI-MS was performed as described previously for membrane proteins (*28*).

*Molecular Weight Determination by SEC Coupled with In-Line Laser Light Scattering, Refractive Index, and Ultraviolet Measurements (SEC-LS/UV/RI).* A Superose-6 HR (10/30) column was coupled with in-line laser light scattering, refraction index (Wyatt Technology, Santa Barbara, CA), and UV (Waters Corp., Milford, MA) detectors (*23*). The system was equilibrated in 20 mM HEPES, pH 7.4, 200 mM NaCl, 1 mM EDTA, 5 mM L-glutamate, and 2 mM DM. Ovalbumin, bovine serum albumin, transferrin, $\beta$-amylase, and apoferritin were used to construct standard curves.

Calculations of molecular weights (MW) were based on the relationships:

$$\left(\frac{dn}{dc}\right)_{pd} = k_2\epsilon\frac{RI}{UV} \quad (1)$$

$$MW = k_1\frac{LS}{\left(\frac{dn}{dc}\right)_{pd}RI} = K\frac{LS\cdot UV}{\epsilon RI^2} \quad (2)$$

The derivative of the refractive index for the protein/detergent complex with respect to protein concentration is $(dn/dc)_{pd}$. LS and RI are the responses from laser light scattering and refraction index detectors, respectively. UV is the response of the UV detector at 280 nm, and $\epsilon$ is the extinction coefficient of the protein in terms of weight concentration ($mg^{-1}$ mL $cm^{-1}$) at 280 nm. The amino acid sequence was used to calculate $\epsilon$ (*27*). The detergent and bound lipids were assumed to have negligible absorbance at 280 nm. For soluble standard proteins $dn/dc$ is constant, and $k_1$, $k_2$, and $K$ parameters can be determined from the standard curves. Molecular weights of the protein components of the protein/detergent complexes were calculated in two ways. First, eq 2, or the so-called "three-detector" method, was used to calculate the molecular weights of the proteins at the elution peak maximum and 90° scattering angle only (*22*). Second, the $(dn/dc)_{pd}$ values were calculated from eq 1, and the protein molecular weights were then determined from the Debye plots in which the light scattering intensity was plotted as a function of the scattering angle (ASTRA software, Wyatt Technology Corp.). The molecular weights were then calculated for thin slices through the entire elution profile (*23*).

*Limited Proteolysis.* His-$GltT_{Bc}$, purified by affinity chromatography and SEC, was digested with bovine trypsin for 30 min at 25 °C in buffer 1 supplemented with 5 mM $CaCl_2$. Reactions were terminated by addition of EDTA and phenylmethanesulfonyl fluoride to 10 and 1 mM final concentrations, respectively. Digested samples were then subjected to MALDI-MS to determine the molecular weights of the resulting fragments. To pinpoint the beginning of each proteolytic fragment, N-terminal amino acid sequencing was performed on protein fragments purified by SDS−PAGE. The determination of fragment identity from respective N-terminal amino acid sequence and molecular weight was aided by the FindPept tool, part of the ExPaSy molecular biology server program collection (*29*).

## RESULTS

*Protein Expression and Purification.* Two approaches were used to express the GltT transporters at high levels: one employed an amino-terminal $His_6$ construct driven by an arabinose promoter in *E. coli* Top10 cells as described previously (*24*); the second utilized a MBP fusion controlled by an IPTG-inducible $P_{tac}$ promoter and DH5α cells (*25*). Both fusion proteins were expressed and accumulated in cell membranes. Purification of His-$GltT_{Bs}$ and His-$GltT_{Bc}$ on Ni-NTA resin followed by SEC gave homogeneous proteins with a yield of about 0.5 mg/L of culture. Replacing the amino-terminal $His_6$ tag with MBP dramatically increased protein expression. However, the MBP fusion exhibited a greater degree of aggregation and proteolytic degradation than the $His_6$-tagged constructs, problems that were subsequently alleviated by reducing the temperature during induction to 22 °C. After purification by affinity chromatography on amylose resin, the protein yields were ca. 2.5 mg/L of culture using MBP fusions.

Removal of the purification tag was critically dependent upon having a linker region between the protease site and the beginning of the native amino terminus. For example, cleavage of the $His_6$ tag of His-$GltT_{Bs}$ using enterokinase failed even though a canonical enterokinase site was present. In contrast, the $His_6$ tag in His-$GltT_{Bc}$ was readily cut by enterokinase. His-$GltT_{Bc}$ had three additional amino acids between the end of the tag and the amino terminus of the transporter, making the enterokinase recognition sequence more accessible. Like enterokinase, TEV protease failed to cleave MBP-SL-$GltT_{Bc}$. However, when a 16 amino acid linker was inserted between the end of the TEV recognition site and the amino terminus of $GltT_{Bc}$ (MBP-LL-$GltT_{Bc}$), TEV cleavage was efficient. Cleaved LL-$GltT_{Bc}$ was purified by SEC, and final protein yields were 0.75−0.9 mg/L of culture.

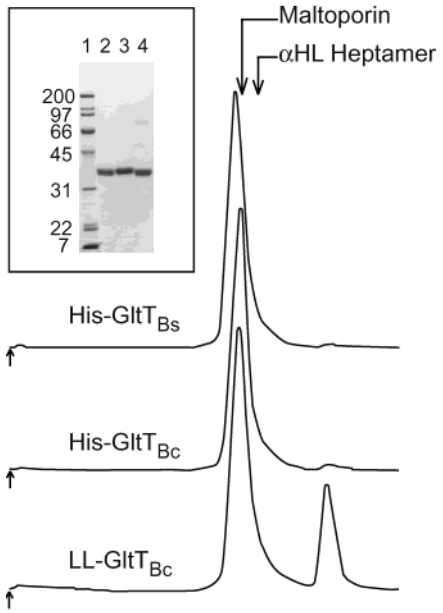


FIGURE 1: Characterization of purified transporters. Analytical SEC of purified transporters on a Superose-6 HR (10/30) column. Arrows indicate points of protein injections. The second peak in the LL-GltT$_{Bc}$ chromatogram contains UV absorbing, small molecular weight substances. The inset shows SDS−PAGE analysis on 12.5% gels. Molecular weight markers are in lane 1 and 4.5 $\mu$g of LL-GltT$_{Bc}$, His-GltT$_{Bc}$, and His-GltT$_{Bs}$ is in lanes 2, 3, and 4, respectively.

Analysis of purified LL-GltT$_{Bc}$, His-GltT$_{Bc}$, and His-GltT$_{Bs}$ by SDS−PAGE is shown in Figure 1. The protein preparations were characterized by a single major band, although there was a faint higher molecular weight band, perhaps corresponding to a His-GltT$_{Bs}$ dimer. The identity and integrity of the transporters were confirmed by N-terminal amino acid sequencing and mass spectrometry. Molecular masses determined by MALDI-MS were 47.16, 47.19, and 46.87 kDa, which were in good agreement with the calculated masses of 47.19, 47.20, and 46.94 kDa for LL-GltT$_{Bc}$, His-GltT$_{Bc}$, and His-GltT$_{Bs}$, respectively.

*SEC Analysis.* GltT proteins eluted on SEC as single peaks (Figure 1), the elution profiles for the three proteins were nearly superimposable, and the traces remained essentially unchanged upon storage for over 2 weeks at 4 °C (data not shown). These results suggested that all three protein preparations were homogeneous and that the proteins were stable and did not aggregate or breakdown over ca. 2 weeks.

*Transport Activity of LL-GltT$_{Bc}$, His-GltT$_{Bc}$, and His-GltT$_{Bs}$ Reconstituted into Liposomes*. To determine that the purified proteins possessed glutamate transport activity, we carried out [$^3$H]glutamate flux experiments according to previously described methods (*20*). Proteins were reconstituted into liposomes at a protein to lipid ratio of 1:400 (w/w). An example of the time course of glutamate accumulation in proteoliposomes is shown in Figure 2. The transport rate at 0.1 $\mu$M external glutamate was ~0.6 nmol of glutamate min$^{-1}$ (mg of protein)$^{-1}$.

*Glutaraldehyde Cross-Linking, SDS−PAGE, and Mass Spectrometry*. To probe the oligomerization state of GltT transporters, we subjected them to glutaraldehyde cross-linking and monitored the reactions by SDS−PAGE and mass spectrometry. Shown in Figure 3 are results analyzed by SDS−PAGE. At lower glutaraldehyde concentrations a small amount of an apparent dimer (band II) was observed while at higher concentrations there was a single major band corresponding to a protein trimer (band III). There was no cross-linking of a SDS-denatured protein, showing that the cross-linking of the native proteins occurred between subunits in an oligomer. A faint high molecular weight band may correspond to a dimer of trimers (band IV). To support the contention that band III was a trimer, cross-linked proteins were subjected to MALDI-MS. The molecular masses determined by mass spectrometry were 147.5, 148.6, and 148.3 kDa, and the calculated trimer masses were 141.57, 141.6, and 140.82 kDa for LL-GltT$_{Bc}$, His-GltT$_{Bc}$, and His-GltT$_{Bs}$, respectively.

*Molecular Weight Determination by SEC-LS/UV/RI*. We also employed a coupled chromatographic and spectroscopic technique that allows one to accurately determine the molecular weights of proteins under nondenaturing conditions. In this technique, a protein sample is applied to an SEC column, and the eluent is passed directly through laser light scattering, refractive index, and UV detectors. The amount of light scattered by a protein solution depends on the protein molecular weight, protein concentration, and the dependence of the refractive index of the solution on protein concentration, d$n$/d$c$. For soluble proteins d$n$/d$c$ is independent of the nature of the protein and is equal to 0.187 mL/g. For membrane proteins that bind an unknown amount of detergent and/or lipid, the dependence of the refractive index on the concentration of the protein/detergent complex, (d$n$/

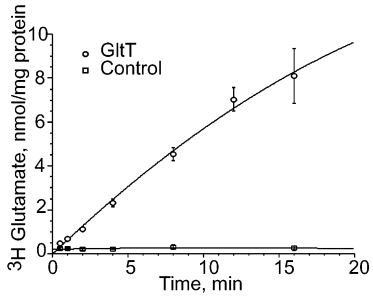


FIGURE 2: [$^3$H]Glutamate uptake by reconstituted His-GltT$_{Bc}$. Circles correspond to the flux into proteoliposomes containing His-GltT$_{Bc}$, and squares correspond to the flux into control liposomes (no transporter). Each point represents an average of two replicates, and the error bars are standard deviations.

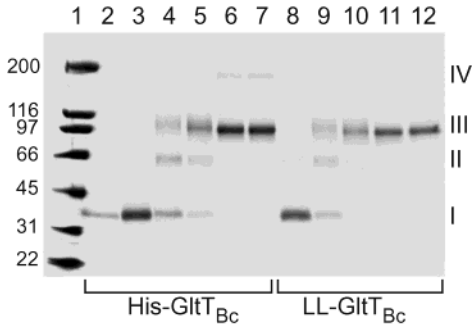


FIGURE 3: Glutaraldehyde cross-linking of His-GltT$_{Bc}$ and LL-GltT$_{Bc}$. Final glutaraldehyde (GA) concentrations were 0.25 mM, lanes 4 and 9; 0.5 mM, lanes 5 and 10; 2.5 mM, lanes 6 and 11; and 5 mM, lanes 7 and 12. SDS was added at 1% concentration to control samples shown in lanes 3 and 8. Molecular weight markers are in lane 1 and His-GltT$_{Bc}$ is in lane 2. Bands I, II, III, and IV correspond to monomer, dimer, trimer, and dimer of trimers, respectively.

Table 1: Oligomerization State of GltT, α-HL, and Maltoporin Determined by SEC-LS/UV/RI

| | MW ($n$)[a] | $(dn/dc)_{pd}$, mL/g[b] | $\delta_s$, g/g of protein[c] |
|---|---|---|---|
| LL-GltT$_{Bc}$ | 140 ± 9 (3.0 ± 0.2) | 0.349 | 1.1 |
| His-GltT$_{Bs}$ | 154 ± 6 (3.3 ± 0.1) | 0.336 | 1.0 |
| α-HL | 226 ± 30 (6.8 ± 0.9) | 0.239 | 0.3 |
| maltoporin | 149 ± 3 (3.2 ± 0.1) | 0.363 | 1.2 |

[a] The molecular weight (MW) and oligomerization state ($n$) were calculated according to the three-detector method; the results are averages from three measurements at three different protein concentrations; errors represent ±1 SD. [b] $(dn/dc)_{pd}$ was calculated according to eq 2. [c] The amount of detergent and lipid bound to the protein was estimated according to eq 3.

$dc)_{pd}$, is determined experimentally by measuring the refractive index of the solution and the protein concentration (*22*, *23*).

Because SEC-LS/UV/RI is a relatively new technique and has only been used to study membrane proteins a few times, we tested the method on the *Staphylococcus aureus* α-HL heptamer and *E. coli* maltoporin (LamB), two very stable, well-characterized membrane proteins with known crystal structures that adopt the same subunit stoichiometry before and following membrane solubilization and purification (*26*, *30*, *31*). The molecular weights calculated using the three-detector method (see eq 2) are shown in the first column of Table 1. The molecular weights and corresponding oligomerization states of α-HL and LamB were within 5−10% of the expected values. When the same method was applied to His-GltT$_{Bs}$ and LL-GltT$_{Bc}$, we obtained results strongly suggesting that the bacterial transporters were trimers (Table 1).

The dependence of the refractive index on protein concentration, $(dn/dc)_{pd}$, is shown in the second column of Table 1. The mass of detergent and lipids bound to the protein was estimated using the relation:

$$\left(\frac{dn}{dc}\right)_{pd} = 0.187 + 0.134\delta_s \qquad (3)$$

Here, 0.187 and 0.134 are the $dn/dc$ values for protein and detergent, respectively (*22*). The $dn/dc$ value for lipids is similar to that for detergent. The mass of detergent and lipid bound to the proteins on a gram per gram basis is defined as $\delta_s$, and the values of $\delta_s$ are shown in the far right column of Table 1. The glutamate transporters and maltoporin bound similar amounts of detergent while α-HL bound approximately 3-fold less detergent.

SEC-LS/UV/RI data were also analyzed using ASTRA software (Wyatt Technology Corp., Santa Barbara, CA) to determine the degree of polydispersity of the protein samples across the elution peaks. Here, one can calculate the molecular weight of the eluted protein at each point of a chromatogram using data from 12 scattering angles. The elution profiles and the molecular weight distributions for LL-GltT$_{Bc}$, α-HL, and maltoporin are shown in Figure 4. The calculated LL-GltT$_{Bc}$ molecular weight was relatively constant across the main peak, suggesting that the protein was monodisperse. A small amount of a larger species eluted earlier in the chromatogram and may correspond to a hexamer, i.e., a dimer of trimers.

*Limited Trypsinolysis*. To map sites on the primary structure of the bacterial transporters that are solvent exposed and flexible, we subjected the proteins to limited proteolysis with trypsin. LL-GltT$_{Bc}$, His-GltT$_{Bc}$, and His-GltT$_{Bs}$ showed similar digestion patterns and susceptibility toward trypsin. An example of a His-GltT$_{Bc}$ digest is shown in Figure 5A.

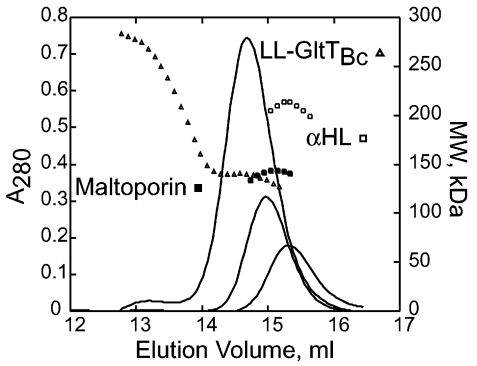


FIGURE 4: ASTRA analysis of SEC-LS/UV/RI data. Calculated molecular weight values for LL-GltT$_{Bc}$ (open triangles), maltoporin (LamB, closed squares), and α-HL (open squares) are plotted. Solid lines correspond to UV traces of the proteins eluting from the SEC column.

The positions of the cleavage sites were determined by a combination of N-terminal amino acid sequencing and MALDI-MS and are indicated in Figure 5B by arrows. The site most susceptible to proteolysis was located shortly after the predicted third transmembrane helix, at the beginning of the large extracellular loop (large arrow in Figure 5B). Cleavage occurred after K108 and after K112, resulting in fragments A and BC. The second and third sites of cleavage were at R276/K288 and K409, resulting in fragments B and C. An additional region within fragment A susceptible to cleavage was located between the second and third transmembrane helices and was defined by lysines 69 and 76, resulting in fragments A1 (∼9.3 kDa) and A2 (∼3.4 kDa). Although A1 did not result in a discrete band on SDS−PAGE, mass spectrometry confirmed its presence, and the N-terminal peptide sequencing of the digest suggested that it was present in an approximate 1:1:1 ratio to the B and C fragments.

## DISCUSSION

There is currently no understanding, at the level of molecular detail, for the ion-dependent cotransport of charged substrates across cell membranes and against concentration gradients. In particular, the molecular mechanism of the high-affinity glutamate transport by glutamate transporters, members of DAACS family, is not known. Moreover, for the bacterial homologues, there is no information on their subunit stoichiometry, and the data that are available on the eukaryotic transporters are contradictory. This lack of consistent information on the most basic element of transporter architecture, coupled with the importance of sodium-dependent, high-affinity glutamate transporters in both prokaryotes and eukaryotes, provides powerful motivations to determine the subunit stoichiometry of the transporters. Even though the most accessible molecules to biochemical and biophysical analysis are clearly the bacterial glutamate transporters, our results are also relevant to the eukaryotic glutamate and neutral amino acid transporters because they share significant amino acid sequence relationships with the sodium-dependent, high-affinity transporters studied here (*7*).

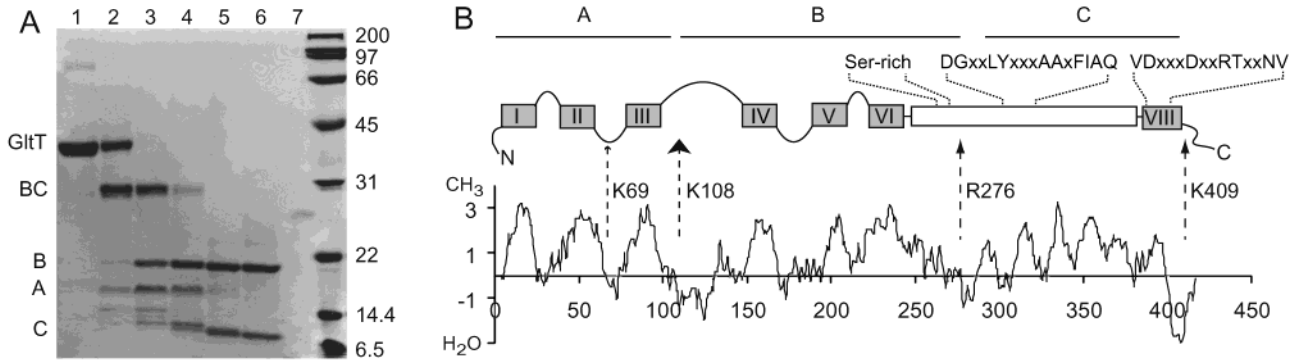


FIGURE 5: Proteolytic digestion pattern and transmembrane topology. (A) Trypsin digest of $(His)_6$-$GltT_{Bc}$. SDS−PAGE of trypsin digests on a 15% gel: lane 1, no trypsin; lanes 2−6, 1:5000, 1:1000, 1:250, 1:50, and 1:10 trypsin to protein ratio (w/w), respectively; lane 7, trypsin (0.6 $\mu$g); lane 8, molecular weight markers. The molecular weights are indicated on the right side of the figure. (B) Hydropathy profile for $GltT_{Bc}$. The profile was generated by the ExPaSy server program ProtScale using a window of nine residues and the hydropathicity scale of Kyte and Doolittle (*47*). Above the profile is the topology model. Solid boxes represent transmembrane helices 1−6 and 8. The membrane-associated region of the transporter with controversial topology is enclosed within an open box. Conserved sequence motifs are shown above the topology model. Arrows indicate trypsin cleavage sites, and the labels A, B, and C correspond to stable trypsin-generated fragments.

The biochemical and biophysical analysis of a glutamate transporter necessarily requires a molecule that is stable to the conditions under which the analysis is carried out. Consequently, one must first find a transporter that maintains its native subunit stoichiometry following membrane solubilization and purification. On the basis of previous work from Konings and colleagues, it was clear that the glutamate transporters from thermophilic bacteria *B. stearothermophilus* and *B. caldotenax* might be suitable molecules. In fact, Konings and co-workers had shown that $GltT_{Bs}$ was substantially more stable than the mesophilic orthologue from *E. coli* and did not require supplementation with lipids and glycerol during purification. Most importantly, $GltT_{Bs}$ retained transport activity during purification under conditions that were very similar to those described here (*20*). Thus, we have concentrated our efforts on $GltT_{Bs}$ and $GltT_{Bc}$.

To optimize the yield of transporter, we explored an alternative expression scheme, in addition to the method previously worked out by Konings et al. (*24*), that involved fusing maltose binding protein to the amino terminus of $GltT_{Bs}$ and $GltT_{Bc}$ (*25*). By using the MBP fusions, we were able to purify approximately twice as much transporter, on a molar basis, in comparison to the $His_6$-tagged constructs. The purified proteins were active in glutamate transport when reconstituted into liposomes, as shown in Figure 2. Previously reported $K_M$ values for $GltT_{Bc}$ and $GltT_{Bs}$ were ca. 30 $\mu$M, and the initial uptake rates for the *E. coli*-expressed, liposome-reconstituted transporters ranged between 4.8 and 6.2 nmol $min^{-1}$ (mg of protein)$^{-1}$ at 1.75 $\mu$M external L-[$^{14}$C]-glutamate (*18*). The rate of uptake measured in the present work, when corrected for the difference in the external glutamate concentration, is similar to that measured by Tolner et al. (*18*). Because the proteins analyzed here have glutamate uptake activity that is similar to that reported in previous studies, and they are homogeneous as judged by SEC, SDS−PAGE, and susceptibility to proteolysis, we contend that they adopt a biologically relevant, native conformation and oligomerization state. Moreover, the proteins remained monodisperse after 2 weeks of storage at 4 °C, and the purification tags did not interfere with the assembly, function, or association state of the transporter.

To some extent, characterization of the oligomerization state of a membrane protein outside of the native lipid bilayer and in detergent micelles is subject to criticism because during the solubilization and purification process, the native state of the protein may be disrupted. However, there are many membrane proteins that retain their native subunit stoichiometry upon membrane solubilization and purification, including the trimeric porins (*32*), heptameric α-hemolysin (*33*), oligomeric light harvesting complexes (*34*), tetrameric Kcsa (*35*, *36*), dimeric BtuCD (*37*), and trimeric AcrB (*38*).

We suggest that $GltT_{Bc}$ and $GltT_{Bs}$ are members of the latter class of membrane proteins that retain their native subunit stoichiometry upon solubilization and purification in mild detergents such as DM. We have shown that, immediately following purification by metal ion affinity chromatography, $GltT_{Bc}$ and $GltT_{Bs}$ migrate as a single peak, corresponding to a trimeric subunit stoichiometry, on a SEC column. This chromatographic behavior is maintained for weeks at 4 °C. Therefore, if the native oligomerization state of $GltT_{Bc}$ and $GltT_{Bs}$ is disrupted by membrane solubilization and purification, it must reach completion by the end of the metal ion affinity chromatography step within 24 h after membrane solubilization, leaving us with a very stable trimer. Thus, even if the native subunit stoichiometry of $GltT_{Bc}$ and $GltT_{Bs}$ is different in the membrane than in detergent micelles, the trimer must be an essential element of the higher order structure in the membrane.

Whether one is working with a purified membrane protein in detergent micelles or a protein in a native membrane, determination of the native oligomerization state is often a challenging task. When working with a detergent-solubilized membrane protein, the bound detergent and lipids greatly complicate canonical methods for determination of native molecular mass, such as sedimentation equilibrium studies in an analytical ultracentrifuge. Although it is possible to perform sedimentation equilibrium studies using a detergent that has a neutral density relative to aqueous solution, such as polyoxyethylene-based detergents (*39*), $GltT_{Bs}$ and $GltT_{Bc}$ are unstable in such detergents. Alternatively, one can "balance" the detergent by using a buffer composed of a mixture of $H_2O$ and $D_2O$ (*40*). Unfortunately, due the partial

specific volume of the detergents in which $GltT_{Bc}$ and $Glt_{Bs}$ are stable, even 100% $D_2O$ is not sufficiently dense to balance the detergent. While one can then turn to other solutes to increase the solution density, these approaches introduce additional problems into the analysis of the centrifugation data. Finally, one can determine the amount of bound detergent using radiolabeled detergent and SEC (*41*). However, this method requires the expensive custom synthesis of the radiolabeled detergent. For these reasons, we decided to pursue two alternative and complementary strategies to determine the subunit stoichiometry of the bacterial glutamate transporters: glutaraldehyde cross-linking coupled with mass spectrometry and SEC-LS/UV/RI.

Glutaraldehyde chemical cross-linking has been successfully used to determine the subunit stoichiometry of water-soluble and membrane proteins (*21*, *42*, *43*), and thus we applied the approach to the characterization of the bacterial glutamate transporters. After reaction of either the $His_6$-tagged $GltT_{Bc}$ and $GltT_{Bs}$ constructs or the cleaved LL-$GltT_{Bc}$ construct, we found that glutaraldehyde cleanly and almost quantitatively cross-linked the bacterial transporter to a trimer. By contrast, glutaraldehyde cross-linking in the presence of SDS did not lead to a higher molecular weight species.

Monitoring the progress of cross-linking was initially carried out by SDS−PAGE. However, membrane proteins and cross-linked membrane proteins frequently demonstrate anomalous mobility during denaturing gel electrophoresis, and therefore molecular mass determination by SDS−PAGE is unreliable. Therefore, to precisely determine the molecular mass of the cross-linked species, we subjected the products of the cross-linking reactions to MALDI-MS (*28*). The experimentally determined masses of the cross-linked species were within 5% of the mass calculated for the trimer. Although the experimental masses were too large by ca. 2−2.5 kDa per protein subunit, this was almost certainly due to the extensive modification of the surface amino groups by glutaraldehyde.

The second method that we employed utilized a relatively novel chromatographic and spectroscopic approach called SEC-LS/UV/RI (*44*, *45*). This method has seen its greatest use in the molecular mass determination of soluble proteins and protein−protein or protein−carbohydrate complexes (*23*). SEC-LS/UV/RI has also been employed, but only in a few instances, for the determination of the molecular masses of detergent-solubilized membrane proteins (*22*). Therefore, we first examined the utility of the SEC-LS/UV/RI method for molecular mass determination of membrane proteins using maltoporin and α-HL as test cases. We chose maltoporin and α-HL not only because they are well characterized and stable in detergent micelles but also because their hydrophobic surface areas are very different, and one would predict that they would bind different amounts of detergent. As shown in Table 1 and Figure 4, application of the SEC-LS/UV/RI method resulted in an accurate determination of the molecular masses of maltoporin and α-HL. In addition, estimation of the mass of detergent bound to maltoporin and α-HL per gram of protein showed that maltoporin bound more detergent, in agreement with the fact that maltoporin has a much larger hydrophobic surface in comparison to α-HL (*41*). Because the SEC-LS/UV/RI method resulted in an accurate determination of the molecular masses and thus the subunit stoichiometry of maltoporin and α-HL, we then applied it to the bacterial glutamate transporters.

The $GltT_{Bc}$ and $GltT_{Bs}$ transporters are trimers as determined using the SEC-LS/UV/RI method and as indicated in Table 1 and Figure 4. Using either the three-detector method, where the molecular mass was determined at the maximum of the elution peak (Table 1), or the so-called ASTRA method, in which the mass was determined at a series of points through the peak (Figure 4), we found similar molecular masses for the $GltT_{Bc}$ and $GltT_{Bs}$ proteins. The measured molecular mass of 140−150 kDa therefore indicated that there are three ∼47 kDa protomers per oligomer. In addition, the results of ASTRA analysis also suggested that the protein samples were monodisperse and that the measured molecular mass was due to the presence of a single species and was not the result of averaging between several species unresolved by SEC.

The trimeric oligomerization state as determined from our studies is consistent with previous cross-linking studies on the eukaryotic GLT-1 (EAAT2) and GLAST (EAAT1) transporters carried out on unpurified proteins in cell membranes. Danbolt and co-workers concluded that trimers and dimers predominated following cross-linking of GLT-1 and GLAST, respectively (*14*). However, because these studies involved the use of crude membrane preparations, they cannot rule out the possibility that they were cross-linking the transporters to other integral membrane proteins. In our study, because we employed purified transporter, the only cross-linked molecules are transporter subunits. Another investigation probing the subunit stoichiometry of glutamate transporters was a low-resolution freeze−fracture study of the EAAT3 transporter overexpressed in *Xenopus* oocytes. In contrast to our results and those of Danbolt and colleagues, the conclusion from the freeze−fracture study was that EAAT3 was a pentamer (*15*). At the present time there is not sufficient information to reconcile our experiments on the bacterial transporters with the electron microscopic work on EAAT3, and in the end it is possible that the assembly state of bacterial and perhaps even eukaryotic transporters is variable. Nevertheless, we would suggest that given the robustness and homogeneity of the $GltT_{Bc}$ and $GltT_{Bs}$ molecules during and after purification, the bacterial transporters are certainly trimers.

To probe the primary structure and solvent accessibility of each subunit within a trimer, we performed limited trypsinolysis. In general, the purified transporters solubilized in DM are relatively resistant to degradation by trypsin, even though there are over 25 lysines and arginines, most of which are localized to putative solvent-exposed loops between the transmembrane segments. Indeed, the substantial resistance of $GltT_{Bc}$ and $GltT_{Bs}$ to degradation by trypsin provides another piece of evidence supporting our contention that they adopt a native conformation during solubilization and purification. Nevertheless, incubation of the transporters with trypsin eventually leads to limited yet specific proteolysis, as shown in Figure 5, yielding the major fragments A, B, and C.

The most reactive site is at the A−B juncture, proximal to the end of the third transmembrane segment and at the beginning of a relatively long hydrophilic segment. This segment comprises the largest extracellular hydrophilic domain of glutamate transporters and is between 40 and 50

residues long in bacterial transporters, and in eukaryotic transporters this region is 25−70 residues longer. Strikingly, despite low sequence conservation, GLT-1 is also susceptible to proteolysis at an equivalent location (*46*), thus providing further evidence for the structural homology between prokaryotic and eukaryotic glutamate transporters. From our proteolysis work, the carboxy-terminal portion of the extracellular loop is protease resistant, suggesting that the domain is well structured. In GLT-1, substrate alters the sensitivity of the protease site proximal to the end of the third transmembrane segment, and thus ligand binding and/or translocation may result in changes in the relative disposition of polypeptide segments A and BC (*46*).

A second but less reactive trypsin site is located between Arg 276 and Lys 288, a few residues after the highly conserved serine-rich motif. The serine-rich motif, defined by Ser 269 and Ser 270 in $GltT_{Bs}$, has been placed at the extracellular end of a transmembrane helix or in the middle of a reentrant loop. Although our experiments did not resolve this controversy, they showed that approximately six residues following the conserved pair of serines there is a flexible and accessible region sensitive to trypsinolysis.

In contrast to the extreme carboxy terminus of the bacterial transporters, where the hydrophilic tail was readily clipped off by trypsin at Lys 409, the amino terminus was highly resistant to proteolysis, despite the presence of Arg 2 and Lys 3 in both $GltT_{Bc}$ and $GltT_{Bs}$. Indeed, effective cleavage of the amino-terminal polyhistidine or MBP tags required the insertion of at least three residues between the protease site and Met 1. These observations suggest that the amino terminus of the transporters is either structured or occluded or both.

## ACKNOWLEDGMENT

We thank Dirk Slotboom and the laboratories of W. N. Konings and J. Lokema for the gift of the *gltT*$_{Bc}$ and *gltT*$_{Bs}$ genes.

## REFERENCES

1. Hille, B. (2001) *Ion channels of excitable membranes*, 3rd ed., Sinauer Associates, Sunderland, MA.
2. Minor, D. L. (2001) *Curr. Opin. Struct. Biol. 11*, 408−414.
3. Amara, S. G., and Fontana, A. C. K. (2002) *Neurochem. Int. 41*, 313−318.
4. Kanner, B. I., and Borre, L. (2002) *Biochim. Biophys. Acta 1555*, 92−95.
5. Slotboom, D. J., Konings, W. N., and Lolkema, J. S. (1999) *Microbiol. Mol. Biol. Rev. 63*, 293−307.
6. Slotboom, D. J., Konings, W. N., and Lolkema, J. S. (2001) *Trends Biochem. Sci. 26*, 534−539.
7. Saier, M. H., Jr. (2000) *Microbiology 146*, 1775−1795.
8. Danbolt, N. C. (2001) *Prog. Neurobiol. 65*, 1−105.
9. Slotboom, D. J. (2001) Thesis, Department of Microbiology, p 92, University of Groningen, Groningen.
10. Seal, R. P., and Amara, S. G. (1999) *Annu. Rev. Pharmacol. Toxicol. 39*, 431−456.
11. Fairman, W. A., Vandenberg, R. J., Arriza, J. L., Kavanaugh, M. P., and Amara, S. G. (1995) *Nature 375*, 599−603.
12. Kanner, B. I., Kavanaugh, M. P., and Bendahan, A. (2001) *Biochem. Soc. Trans. 29*, 707−710.
13. Slotboom, D. J., Konings, W. N., and Lolkema, J. S. (2001) *FEBS Lett. 492*, 183−186.
14. Haugeto, O., Ullensvang, K., Levy, L. M., Chaudhry, F. A., Honore, T., Nielsen, M., Lehre, K. P., and Danbolt, N. C. (1996) *J. Biol. Chem. 271*, 27715−27722.
15. Eskandari, S., Kreman, M., Kavanaugh, M. P., Wright, E. M., and Zampighi, G. A. (2000) *Proc. Natl. Acad. Sci. U.S.A. 97*, 8641−8646.
16. de Vrij, W., Bulthuis, R. A., van Iwaarden, P. R., and Konings, W. N. (1989) *J. Bacteriol. 171*, 1118−1125.
17. Heyne, R. I. R., de Vrij, W., Crielaard, W., and Konings, W. N. (1991) *J. Bacteriol. 173*, 791−800.
18. Tolner, B., Poolman, B., and Konings, W. N. (1992) *Mol. Microbiol. 6*, 2845−2856.
19. Tolner, B., Ubbink-Kok, T., Poolman, B., and Konings, W. N. (1995) *Mol. Microbiol. 18*, 123−133.
20. Gaillard, I., Slotboom, D. J., Knol, J., Lolkema, J. S., and Konings, W. N. (1996) *Biochemistry 35*, 6150−6156.
21. Peters, K., and Richards, F. M. (1977) *Annu. Rev. Biochem. 46*, 523−551.
22. Hayashi, Y., Matsui, H., and Takagi, T. (1989) *Methods Enzymol. 172*, 514−528.
23. Folta-Stogniew, E., and Williams, K. R. (1999) *J. Biomol. Technol. 10*, 51−63.
24. Slotboom, D. J., Sobczak, I., Konings, W. N., and Lolkema, J. S. (1999) *Proc. Natl. Acad. Sci. U.S.A. 96*, 14282−14287.
25. Sheffield, P. J., Garrard, S., and Derewenda, Z. (1999) *Protein Expression Purif. 15*, 34−39.
26. Song, L., Hobaugh, M. R., Shustak, C., Cheley, S., Bayley, H., and Gouaux, J. E. (1996) *Science 274*, 1859−1866.
27. Pace, C. N., Vajdos, F., Fee, L., Grimsley, G., and Gray, T. (1995) *Protein Sci. 4*, 2411−2423.
28. Cadene, M., and Chait, B. T. (2000) *Anal. Chem. 72*, 5655−5658.
29. Gattiker, A., Bienvenut, W. V., Bairoch, A., and Gasteiger, E. (2002) *Proteomics 2*, 1435−1444.
30. Lepault, J., Dargent, B., Tichelaar, W., Rosenbusch, J. P., Leonard, K., and Pattus, F. (1988) *EMBO J. 7*, 261−268.
31. Schirmer, T., Keller, T. A., Wang, Y.-F., and Rosenbusch, J. P. (1995) *Science 267*, 512−514.
32. Schulz, G. E. (1996) *Curr. Opin. Struct. Biol. 6*, 485−490.
33. Bhakdi, S., Füssle, R., and Tranum-Jensen, J. (1981) *Proc. Natl. Acad. Sci. U.S.A. 78*, 5475−5479.
34. Nunn, R. S., Artymiuk, P. J., Baker, P. J., Rice, D. W., and Hunter, C. N. (1992) *J. Mol. Biol. 228*, 1259−1262.
35. Heginbotham, L., Odessey, E., and Miller, C. (1997) *Biochemistry 36*, 10335−10342.
36. Doyle, D. A., Cabral, J. M., Pfuetzner, R. A., Kuo, A., Gulbis, J. M., Cohen, S. L., Chait, B. T., and MacKinnon, R. (1998) *Science 280*, 69−77.
37. Locher, K. P., Lee, A. T., and Rees, D. C. (2002) *Science 296*, 1091−1098.
38. Murakami, S., Nakashima, R., Yamashita, E., and Yamaguchi, A. (2002) *Nature 419*, 587−593.
39. Fleming, K. G., Ackerman, A. L., and Engelman, D. M. (1997) *J. Mol. Biol. 272*, 266−275.
40. Edelstein, S. J., and Schachman, H. K. (1967) *J. Biol. Chem. 242*, 306−311.
41. Moller, J. V., and le Maire, M. (1993) *J. Biol. Chem. 268*, 18659−18672.
42. Maduke, M., Pheasant, D. J., and Miller, C. (1999) *J. Gen. Physiol. 114*, 713−722.
43. Canals, F. (1992) *Biochemistry 31*, 4493−4501.
44. Wen, J., Arakawa, T., and Philo, J. S. (1996) *Anal. Biochem. 240*, 155−166.
45. Stuting, H. H., and Krull, I. S. (1990) *Anal. Chem. 62*, 2107−2114.
46. Grunewald, M., and Kanner, B. I. (1995) *J. Biol. Chem. 270*, 17017−17024.
47. Kyte, J., and Doolittle, R. F. (1982) *J. Mol. Biol. 157*, 105−132.

BI030161Q